

is only a matter of a few percent and is negligible. The above phenomenon is illustrated in Fig. 4. The monovalent positive ion would be expected to exhibit a symmetrical behavior.

The induced polarization of neighboring neutral molecules by the molecule ion has not been studied quantitatively. However, our intuitive feeling is that the delocalization of the extra π electron should substantially reduce the polarization of its environment,

and that the reaction of this polarization back on the electron should be small.

Although other molecules should be examined in this connection if sufficient information is available, it is physically reasonable to assume that the above conclusions apply to organic molecules of comparable or larger size. This may not be true for smaller diatomic molecules (such as iodine), or for those possessing a permanent dipole moment, e.g., $[(TCNQ)^-M^+]$.

Optical and Electrical Properties and Energy Band Structure of ZnSb*

H. KOMIYA,[†] K. MASUMOTO,[‡] AND H. Y. FAN

Purdue University, Lafayette, Indiana

(Received 11 October 1963)

Single crystals of p -type ZnSb have been grown by pulling from the melt. The carrier concentration is of the order of 10^{16} cm⁻³. The Hall mobility is of the order of a few hundred cm²/sec-V at room temperature, and is highest for current along the c axis and lowest for current along the b axis. Indirect and direct transitions have been observed in the absorption edge. The indirect transitions begin at the photon energy: 0.50 eV at 300°K, 0.59 eV at 77°K, and 0.61 eV at 4.2°K, independent of polarization. The direct transitions appear to begin at the lowest photon energy for $E||c$ and at the highest photon energy for $E||a$. The carrier absorption at long wavelengths is highest for $E||c$. The results indicate that the valence band has three closely spaced bands near the maximum which corresponds to either the point Γ or the points R of the Brillouin zone, while the minimum of the conduction band is at the other position. The effective mass tensor of holes is estimated.

INTRODUCTION

TWO II-V semiconducting compounds, CdSb and ZnSb, have similar crystal structures of orthorhombic symmetry. Being noncubic, these crystals may have interesting anisotropic properties which help to elucidate the structure of the electronic energy bands. Early studies made on polycrystalline material of ZnSb emphasized the thermal and thermoelectric properties which were of interest for technical application of the material. Recently, some investigations of optical and electrical properties have been made on single crystals of CdSb, Zn _{x} Cd _{$1-x$} Sb as well as ZnSb. Most studies were made on p -type material; a few measurements were made on n -type CsSb. Anisotropy in conductivity and Hall coefficient has been reported for CdSb by Adronik and Kot¹ and for ZnSb by Kot and Kretsu²; the axes of the crystal were not identified.

Štourač, Tauc, and Závětová³ found that $\sigma_c > \sigma_b$ in the CdSb, Zn_{0.23}Cd_{0.77}Sb and Zn_{0.25}Cd_{0.75}Sb crystals studied; the authors also studied the infrared absorption edge in these crystals and found a difference in the absorption for different polarizations. The absorption was interpreted as due to indirect transitions. The absorption edge in CdSb was measured also by Trei *et al.*⁴ with polarized radiation and was also attributed to indirect transitions. The latter authors studied also magnetoresistance of n - and p -type CdSb. They postulated for CdSb a model with one type of holes and one type of electrons and found that constant energy ellipsoid for electrons as well as for holes have axes along the crystal axes. For ZnSb, absorption edge measurements have been reported by Turner, Fischler, and Reese⁵ for unpolarized radiation only. The measurements were made on p -type samples with rather high carrier concentrations, $\sim 4 \times 10^{18}$ cm⁻³. From the measurements, the energy gap at room temperature was estimated to be approximately 0.53 eV. Finally,

* Work supported by an Advanced Research Projects Agency Contract and an U. S. Army Research Office Contract.

[†] Present address: Physics Department, Mitsubishi Research Laboratory, Hyogo, Japan.

[‡] Present address: 14 3-Chrome Toshima-ku, Tokyo, Japan.

¹ I. K. Andronik and M. V. Kot, *Fiz. Tverd. Tela* **1**, 1128 (1960) [English transl.: *Soviet Phys.—Solid State* **2**, 1022 (1960)]; see also I. K. Andronik, M. V. Kot, and M. V. Emelyanenko, *Fiz. Tverd. Tela* **3**, 2548 (1961) [English transl.: *Soviet Phys.—Solid State* **3**, 1853 (1962)].

² M. K. Kot and I. V. Kretsu, *Fiz. Tverd. Tela* **2**, 1250 (1960) [English transl.: *Soviet Phys.—Solid State* **2**, 1134 (1960)].

³ L. Štourač, J. Tauc, and M. Závětová, *Proceedings of the International Conference on Semiconductor Physics, 1960* (Czechoslovakian Academy of Sciences, Prague, 1961), p. 1091.

⁴ V. Trei, M. Matyáš, B. Velický, and M. Závětová, *Proceedings of the International Conference on the Physics of Semiconductors, Exeter* (The Institute of Physics and the Physical Society, London, 1962), p. 766.

⁵ W. J. Turner, A. S. Fischler, and W. E. Reese, *Phys. Rev.* **121**, 759 (1961).

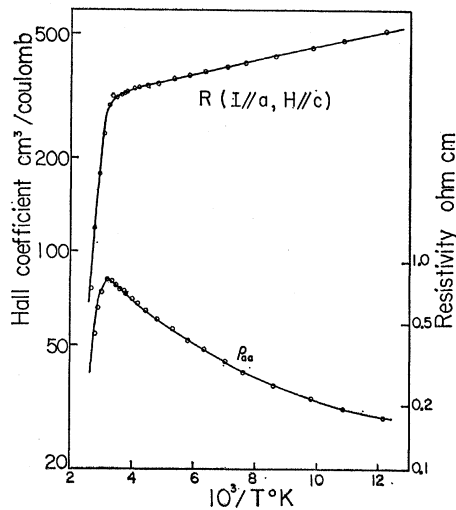


FIG. 1. Hall coefficient and resistivity as functions of reciprocal temperature. The current was along the a axis.

cyclotron resonance measurements on p -type CdSb and p -type ZnSb have been reported by Stevenson⁶ using optical excitation. Effective mass values obtained are $0.140m$ along the b axis and isotropic, $0.159m$, in the a - c plane for CdSb, and $0.175m$ along the a axis and isotropic, $0.146m$, in the b - c plane for ZnSb. The sign of the charge of the carrier was not determined. It seems likely that the results pertain to holes.

The brief summary shows that the experimental data on these crystals are as yet far from adequate for obtaining detailed information on the energy band structure. In the following, optical and some electrical studies on single crystals of ZnSb are reported. The optical studies were made with polarized radiations.

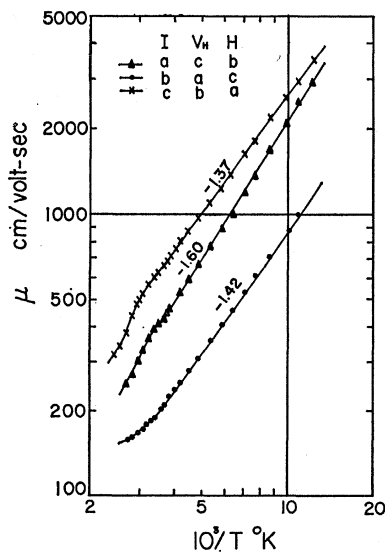


FIG. 2. Temperature dependence of Hall mobility. Data are shown for three samples, each with current along a different axis.

⁶ M. J. Stevenson, *Proceedings of the International Conference on Semiconductor Physics, 1960* (Czechoslovakian Academy of Sciences, Prague, 1960), p. 1083.

Information on the energy band structure is derived from the results.

EXPERIMENTAL RESULTS

Single crystals were obtained by pulling from the melt. No doping impurities were introduced. The crystals obtained were p -type. The lattice dimensions of ZnSb crystal are known to be: $a=6.218 \text{ \AA}$, $b=7.741 \text{ \AA}$, and $c=8.115 \text{ \AA}$. Representative curves of resistivity and Hall coefficient are shown in Fig. 1 for current along the a axis. The curves are similar for current along the other axes. The temperature dependence of the Hall mobility is shown in Fig. 2. The data show that the conductivity and Hall mobility are highest for current along the c axis and lowest for current along the b axis. The data shown for different current directions were actually obtained on different samples, however the conclusion about the anisotropy is based on measurements on several samples for each current direction. The results of Andronik and Kot^{1,2} and Štourač *et al.*³ indicate that qualitatively the same anisotropy exists also in CdSb and the solid solutions of ZnSb and CdSb. The temperature dependence of the Hall mobility is close to $T^{-1.5}$ and appears to be somewhat stronger for current along the a axis than for current along the b and c axes. It seems that acoustic modes of lattice vibration are the dominant scattering mechanism in these crystals. The steep slopes at the high-temperature end of the resistivity and Hall coefficient curves apparently correspond to intrinsic conduction. From the data, a value of $E_0=0.57 \text{ eV}$ is estimated using the approximation, $E_G=E_0+aT$, for the energy gap in this temperature range. Heating at temperatures above 200°C produces changes in the electrical properties measured at lower temperatures. Such effect was reported by Kot and Kretsu² who attributed it to the thermal dissociation of the crystal. Some preliminary measurements were made on the thermoelectric power. At room temperature, the values measured are around $500 \mu\text{V}/^\circ\text{C}$.

ABSORPTION EDGE

The refractive index for infrared radiation was determined by using interference in transmission through thin samples. Figure 3 gives the results for radiations polarized along each of the three crystal axes. These results are used for the calculation of absorption from transmission measurements.

The absorption edges for the three directions of polarization are shown in Fig. 4 for the ambient and liquid-helium temperatures. The absorption begins to rise at the same photon energy independent of the polarization. By extrapolation, after subtracting the flat absorption at low energies, we get threshold energies; $E_t=0.50, 0.59, \text{ and } 0.61 \text{ eV}$ for the three temperatures $300, 77, \text{ and } 4.2^\circ\text{K}$, respectively. At high photon energies, the absorption rises more steeply

before it bends to flatten. The change over to steeper rise is clearly evident in the low-temperature curves. We interpret the steep rise as caused by direct transitions. The more sloping absorption at smaller photon energies is then produced by indirect transitions, and is seen to be smaller at lower temperatures as expected. The threshold for direct transitions appears to be different for different directions of polarization. It is difficult to determine accurately the thresholds for direct transitions due to the superposition of indirect transitions. At an absorption level of 3500 cm^{-1} , we get 1.11 eV for $E||a$, 1.09 eV for $E||b$, and 1.05 eV for $E||c$ at 4.2°K. At room temperature, the same absorption corresponds to 0.99 eV for $E||a$. For the two other polarizations, the energy shift between the two temperatures appears to be larger which may be partly due to the larger admixture of indirect transitions at room temperature. We have not yet succeeded in observing in the indirect absorption fine structures marking thresholds of phonon absorption and emission processes. These thresholds are necessary for the precise determination of the energy gap. However, the values of threshold energy E_s given above serve as fair estimates of the energy gap to within 0.02–0.03 eV.

The low-temperature absorption curves for $E||b$ show a peak at 0.72 eV. It was found that the peak depended on the preparation of the sample surfaces and could be almost eliminated by exercising extra care in all stages of the polishing operation. The absorption peak was apparently produced by a damaged

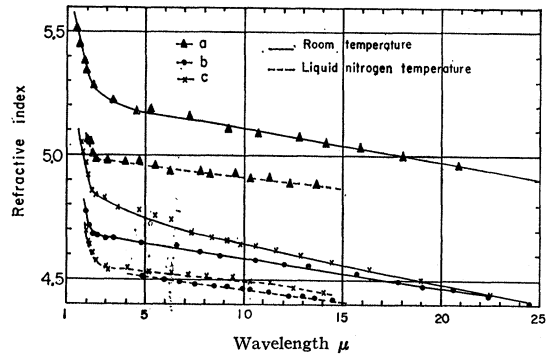


FIG. 3. Refractive indices as functions of wavelength for polarized radiations.

surface layer. It is interesting that the surface layer produced extra absorption only for $E||b$. For $E||a$, some samples gave at low temperatures an absorption hump in the region 1.0–1.1 eV. Other samples did not give a hump and the data followed the dashed lines. It is not certain whether the hump was also produced by a surface layer.

LONG-WAVELENGTH ABSORPTION

Measurements were made up to 30μ . Figure 5 shows an absorption curve for each polarization. Below 0.1 eV, the absorption increased smoothly with decreasing photon energy. For $E||c$, the absorption varied approximately as ν^{-2} and the magnitude varied among

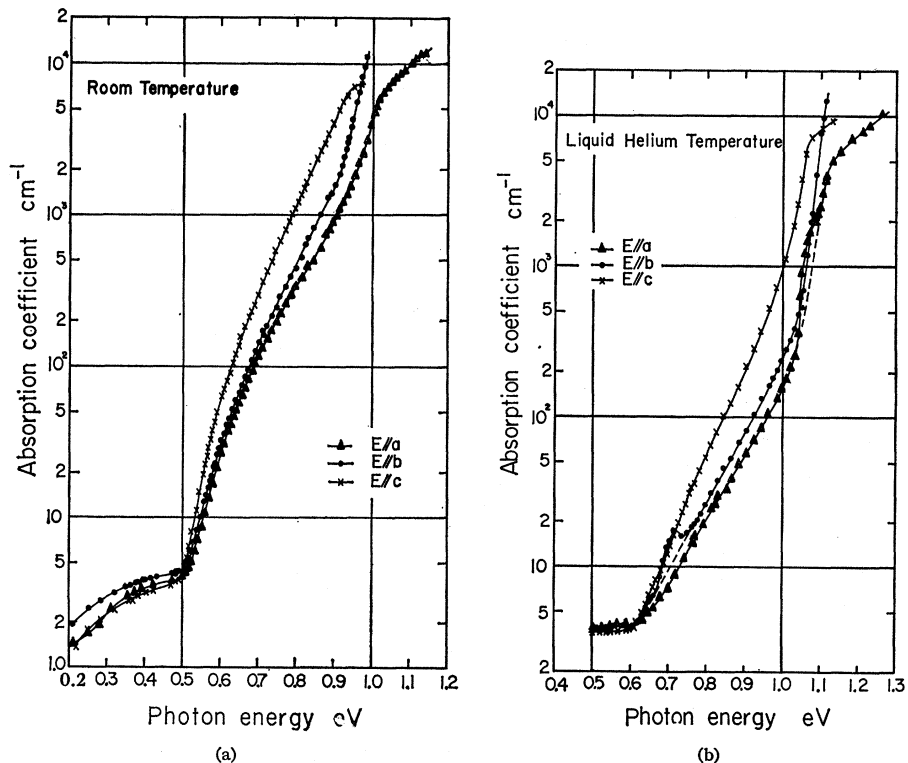


FIG. 4. (a) Absorption edges for polarized radiations, at room temperature. (b) Absorption edges for polarized radiation, at liquid-helium temperature.

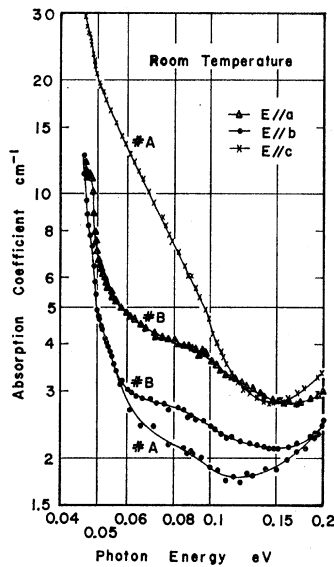


FIG. 5. Curves of absorption coefficient for polarized radiations. Data shown were obtained on two samples, A and B.

samples. It is evidently free-carrier absorption. The curves show that free-carrier absorption is much lower for the other two polarizations.

A number of absorption bands were observed below 0.05 eV. Figure 6(a) shows the data taken on two samples. The absorption bands are not all the same for the three directions of polarization. Comparing the two curves for $E||c$, we see that one of the samples has generally higher absorption having apparently a higher carrier absorption. The magnitude of the absorption bands is, however, about the same. Furthermore, the magnitudes of the absorption bands decreased with decreasing temperature as can be seen in Fig. 6(b). These observations indicate that the absorption bands are associated with lattice vibrations. The data in

Fig 6(b) show that there is a small shift of the absorption bands toward higher energy at the lower temperature. With sixteen atoms per unit cell,⁷ the lattice vibration has many branches. It is planned to extend the measurements to longer wavelengths in order to study the full lattice absorption spectrum.

The absorption shown in Fig. 5 increases with photon energy in the region from 0.15 eV to the absorption edge. Figure 7 shows that there is no significant change of the absorption spectrum with temperature in contrast to the interband transition of holes in germanium. We attribute this absorption to an impurity level about 0.13 eV from the valence band. The absorption is produced by the excitation of electrons from the valence band to this level. It is most likely an acceptor level and its position would be fixed relative to the valence band. The threshold of this absorption does not therefore shift with the temperature variation of the energy gap. It can be easily seen from the Hall coefficient curve in Fig. 1. that the level in question can not be the residual acceptor level that is responsible for the p -type conduction. The nature of the impurity or lattice defect is unknown. To some extent, the absorption is present in all the samples studied. In his cyclotron resonance work on p -type ZnSb, Stevenson⁶ used infrared excitation and found that resonance signal was absent when the photon energy of the infrared light was less than 0.2 eV. The level in question may be responsible for the excitation of holes with photon energy less the energy gap.

DISCUSSION

The crystal lattice of ZnSb and CdSb belongs to the D_{2h}^{15} space group⁷ having twofold screw axes C_{2x} , C_{2y} , C_{2z} parallel to the crystal axes, glide planes σ_x , σ_y , σ_z

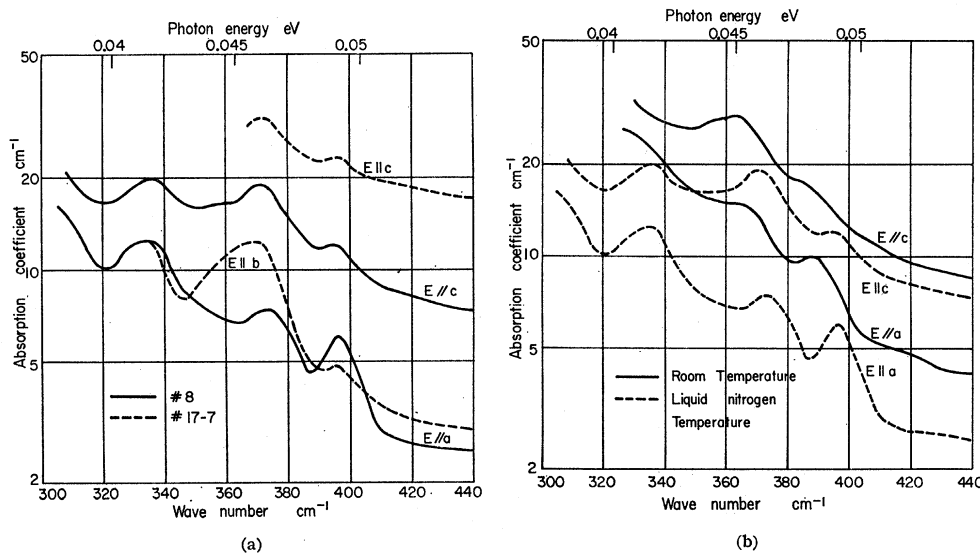


FIG. 6. (a) Absorption curves for polarized radiations, showing absorption bands. The solid curves show the data obtained on one sample and the dashed curves show the data for another sample. (b) Absorption curves showing the variation of absorption bands with temperature.

⁷ K. E. Almin, Acta Chem. Scand. 2, 400 (1948); K. Toman, Phys. Chem. Solids 16, 160 (1960).

perpendicular to the axes, and inversion centers I . The Brillouin zone is a rectangular parallelepiped. The representations of the symmetry points of the Brillouin zone have been worked out by Khartsiev.⁸ Table I reproduces the character table of the representations for the center, Γ , of the Brillouin zone. For the points R at the corners of the Brillouin zone, the representations of the simple group, R_1 and R_2 , coincide with the additional representations of the double group for Γ , and the additional double groups representations, R_3 to R_{10} , coincide with the simple group representations Γ_1 to Γ_8 .

We shall consider the implications of the experimental results making as few assumptions as possible. Khartsiev has examined the energy gradient along different directions of \mathbf{k} for the symmetry points and points on symmetry lines. In the simple group as well as in the double group representations, only the Γ and R points have zero gradients in all three directions k_x , k_y , and k_z . Since the absorption begins with indirect transitions, this indicates that one of the band edges is at Γ while the other band edge corresponds to the points R . Direct transitions may begin either at Γ or R . The three thresholds observed for different polarizations indicate that the transitions begin at the point where one of the bands has three closely spaced branches. We denote the three branches by T_c , T_b , and T_a . The edge of the other band at that point will be denoted by S . The group of Γ and that of R contain the inversion element, and the representations may be characterized by parity. So far as the experimental results are concerned, S may be any one of the representations of Γ or of R . The representations of T bands must have the parity opposite to that of S . Thus, direct transitions are not allowed between any two T 's. For example, if S has the representation Γ_5 then T_c , T_b , T_a may have Γ_4 , Γ_2 , Γ_3 , respectively, with Γ_4 giving transitions for $E||c$, Γ_2 giving transitions for $E||b$, and Γ_3 giving transitions for $E||a$. This is, however, not the only possibility. Any and all of the three representations, Γ_2 , Γ_3 , and Γ_4 , may be replaced by Γ_9 , which has zero character for many of the symmetry elements.

Let \mathbf{k}_0 be the wave number corresponding to T and S . The selection rules making only one particular polarization effective for each T apply only at \mathbf{k}_0 . For photon energies above the threshold, the discrimination regarding polarization is relaxed. To consider wave functions $\mathbf{k}=\mathbf{k}_0+\Delta\mathbf{k}$, we shall use as usual the perturbation approach,⁹ the Bloch wave function for \mathbf{k} may be written¹⁰:

$$\psi_{n\mathbf{k}} = e^{i\Delta\mathbf{k}\cdot\mathbf{r}} (e^{i\mathbf{k}_0\cdot\mathbf{r}} U_{n\mathbf{k}}) \equiv e^{i\Delta\mathbf{k}\cdot\mathbf{r}} \varphi_{n\mathbf{k}}, \quad (1)$$

$\varphi_{n\mathbf{k}_0}$ being the Bloch wave function for \mathbf{k}_0 . Substitution of the expression reduces the Schrodinger equation to

⁸ V. E. Khartsiev, Fiz. Tverd. Tela 4, 893 (1962) [English transl.: Soviet Phys.—Solid State 4, 121 (1962)].

⁹ E. O. Kane, Phys. Chem. Solids 1, 249 (1957).

¹⁰ J. M. Luttinger and W. Kohn, Phys. Rev. 97, 869 (1955).

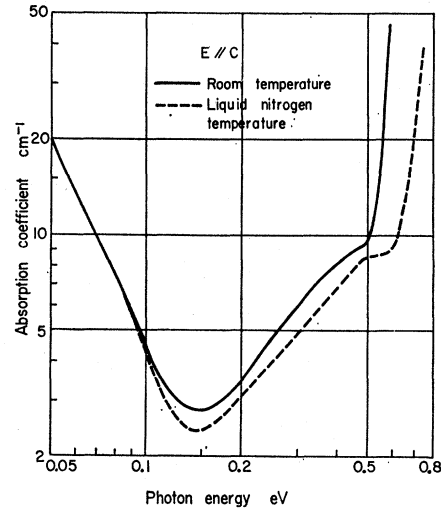


FIG. 7. Absorption curves in the region of impurity absorption, for room temperature and liquid-nitrogen temperature.

an equation for $\varphi_{n\mathbf{k}}$ in which the Hamiltonian operator contains a term dependent on $\Delta\mathbf{k}$:

$$H' = -\frac{\hbar}{m} \Delta\mathbf{k} \cdot \left(\mathbf{p} - \frac{\hbar}{4mc^2} \nabla V \times \boldsymbol{\sigma} \right) \equiv -\frac{\hbar}{m} \Delta\mathbf{k} \cdot \boldsymbol{\pi}, \quad (2)$$

where $\boldsymbol{\sigma}$ is the Pauli spin vector, V is the crystalline potential, and $\boldsymbol{\pi}$ is referred to as the modified momentum operator which contains an additional term coming from spin-orbit interaction. The spin-orbit interaction also contributes a $\Delta\mathbf{k}$ independent term to the Hamiltonian operator but this term is included in the unperturbed Hamiltonian to give the double group representations, $\psi_{n\mathbf{k}_0}$'s. We treat H' as perturbation taking into account only the bands S and T 's. The unperturbed functions are $\varphi_{n\mathbf{k}_0} = \psi_{n\mathbf{k}_0}$. Parity consideration shows that the operator $\boldsymbol{\pi}$ has zero-matrix elements between any two of the T bands. For the matrix elements between the S and the various T bands, $\boldsymbol{\pi}$ may

TABLE I. Character table (Ref. 8) of simple and double group representations for the point Γ .

Γ	E	Simple group representations						
		C_{2x}	C_{2y}	C_{2z}	1	σ_x	σ_y	σ_z
1	1	1	1	1	1	1	1	1
2	1	-1	1	-1	1	-1	1	-1
3	1	1	-1	-1	1	1	-1	-1
4	1	-1	-1	1	1	-1	-1	1
5	1	1	1	1	-1	-1	-1	-1
6	1	-1	1	-1	-1	1	-1	1
7	1	1	-1	-1	-1	-1	1	1
8	1	-1	-1	1	-1	1	1	-1

Additional representations of the double group

Γ	E	\bar{E}	I	\bar{I}
9	2	-2	2	-2
10	2	-2	-2	2

Characters of other elements are zero

be replaced approximately by \mathbf{p} . We get then for the S band:

$$\begin{aligned}\varphi_{sk} &= \varphi_{sk_0} + \frac{\hbar}{m} \sum_i \frac{1}{E_s - E_i} \Delta k_i (p_i)_{is} \varphi_{ik_0}, \\ E_{sk} &= E_{sk_0} + \frac{\hbar^2}{2m} (\Delta k)^2 + \frac{\hbar^2}{m^2} \sum_i \frac{|(p_i)_{is}|^2}{E_s - E_i} (\Delta k_i)^2,\end{aligned}\quad (3)$$

where the subscript i is the running index for the three bands T_a , T_b , T_c or the three directions along the crystal axes a , b , c . The expressions for the three T bands may be written:

$$\begin{aligned}\varphi_{ik} &= \varphi_{ik_0} + \frac{\hbar}{m} \frac{1}{E_i - E_s} \Delta k_i (p_i)_{si} \varphi_{sk_0}, \\ E_{ik} &= E_{ik_0} + \frac{\hbar^2}{2m} (\Delta k)^2 + \frac{\hbar^2}{m^2} \frac{|(p_i)_{si}|^2}{E_i - E_s} (\Delta k_i)^2.\end{aligned}\quad (4)$$

Any of the bands may be degenerate, having one of the two dimensional representations of Γ or R . This possibility does not give rise to serious complication in the perturbation treatment since H' has no matrix element between the degenerate states.

The departure from the selection rule for $\mathbf{k}=\mathbf{k}_0$ depends both on the admixture of φ_{ak_0} , φ_{bk_0} , and φ_{ck_0} in φ_{sk} and the admixture of φ_{sk_0} in φ_{ak} , φ_{bk} , and φ_{ck} . For example, transitions produced by $E||b$ between T_c and S depends on the matrix element:

$$\int \Delta \varphi_{ck}^* p_b \Delta \varphi_{sk} \propto \Delta k_c \Delta k_b \int \varphi_{sk_0}^* p_b \varphi_{bk_0}. \quad (5)$$

For small Δk , such transitions will be weak so that the effect near the thresholds of direct transitions may be obscured by the indirect transitions.

Consider now the experimental results on dc conductivity and infrared carrier absorptions. The dc mobility tensor has components $\mu_c > \mu_a > \mu_b$ indicating that $\tau_c/m_c > \tau_a/m_a > \tau_b/m_b$, where τ_a , τ_b , τ_c and m_a , m_b , m_c are the tensor components of relaxation time and effective mass of holes. The infrared absorption of free

carriers shows that $\alpha_c > \alpha_b \gtrsim \alpha_a$. As pointed out, α_b and α_a could not be estimated reliably. Taking into account the difference in refractive index n , we can conclude with certainty about the infrared conductivity, $\sigma = 4\pi\alpha/cn$, that $\sigma_c > \sigma_b$ and $\sigma_c > \sigma_a$. In the Drude-Kronig theory, the conductivity is given by:

$$\sigma = \sigma_0 / [1 + (\omega\tau)^2] \propto 1/m^*\tau \quad (6)$$

with the approximation applying for $\omega\tau \gg 1$. The same dependence on $m^*\tau$ is given also by quantum treatment of carrier absorption with phonon assistance.¹¹ The dc and infrared data indicated that the effective mass has a distinctly smaller component along the c axis. The cyclotron resonance results reported by Stevenson⁶ give $m_a = 0.175 m$ and $m_b = m_c = 0.146 m$ which probably pertain to holes. The tentative estimate we get is, on the other hand, $m_c \sim 0.05 m$, $m_b \sim 0.6 m_a$.

Our results about the effective mass suggest that the three T bands are at the maximum of the valence band, with T_c having the highest and T_a the lowest energy. Since T_c is separated from the next lower band T_b by ~ 0.04 eV, it predominates in the p -type conduction at room temperature and lower temperatures. Equation (4) shows that the effective mass for the T_c band is expected to have a smaller component along c axis due to interaction with the S band. We have as yet no experimental indication about which of the two, the maximum of the valence band and the minimum of the valence band, is at Γ and which is at R . Regarding ZnSb as comparable to Ge and α -Sn, with lattice deformed slightly from the O_h ⁷ symmetry to the D_{2h} ¹⁵ symmetry, Khartsiev^{8,12} suggested that the lowest conduction band has $\Gamma_5(\Gamma_{10})$ at $k=0$ corresponding to $\Gamma_2'(\Gamma_{7-})$ in germanium while the valence band has three branches $\Gamma_2(\Gamma_9)$, $\Gamma_3(\Gamma_9)$, $\Gamma_4(\Gamma_9)$ corresponding to $\Gamma_{25}'(\Gamma_{8+}$ and $\Gamma_{7+})$ in germanium. Double group representations are given in brackets. While such a model is qualitatively compatible with the observed results, further investigations are necessary to verify the suggestion.

¹¹ H. Y. Fan, Rept. Progr. Phys. **16**, 107 (1956).

¹² V. E. Khartsiev, Fiz. Tverd. Tela **5**, 1225 (1963) [English transl.: Soviet Phys.—Solid State **5**, 894 (1963)]; we are indebted to Dr. Khartsiev for a reprint of the paper.